*Nigerian Journal of Technology (NIJOTECH)*
*Vol. 44, No. 1, March, 2025, pp.77 - 86*
*www.nijotech.com*

*Print ISSN: 0331-8443*
*Electronic ISSN: 2467-8821*
*https://doi.org/10.4314/njt.v44i1.9*

# THERMOACOUSTIC COOLING PERFORMANCE USING NYLON 6 STACK MATERIAL OF VARIED GEOMETRY AND BLENDED HELIUM-ARGON GAS

**AUTHORS:**
K. S. Shelke[1], U. S. Wankhede[2], and S. Shelare[3,*]

**AFFILIATIONS:**
[1]Mechanical Engineering, Government College of Engineering Chandrapur, Maharashtra, 442403 India.
[2]Mechanical Engineering, Government College of Engineering, Nagpur, Maharashtra, 441108, India.
[3]Mechanical Engineering, Priyadarshini College of Engineering, Nagpur, Maharashtra, 440019, India
[3]Centre for Research Impact and Outcome, Chitkara University Institute of Engineering and Technology, Chitkara University, Rajpura 140401, Punjab, India
[3]Department of Technical Sciences, Western Caspian University, Baku, Azerbaijan

***CORRESPONDING AUTHOR:**
Email: *sagmech24@gmail.com*

**ARTICLE HISTORY:**
**Received:** 11 October, 2024.
**Revised:** 21 February, 2025.
**Accepted:** 27 February, 2025.
**Published:** 14 April, 2025.

**KEYWORDS:**
Gas mixture, Nylon 6, Performance, Thermoacoustic refrigeration.

**ARTICLE INCLUDES:**
Peer review

**DATA AVAILABILITY:**
On request from author(s)

**EDITORS:**
Chidozie Charles Nnaji

**FUNDING:**
None

## Abstract

*Meeting the increased demand for energy-efficient, eco-friendly cooling technology requires innovative materials and gas combinations. Conventional cooling systems employ harmful refrigerants that cause global warming and ozone depletion. Thermal and acoustic nylon 6 is a potential stack material for thermoacoustic cooling systems. Despite the potential of Nylon 6 in thermoacoustic applications, its performance with different stack geometries and gas mixtures remains underexplored. Investigating the synergistic effects of these gas combinations has the potential to increase the efficiency and cooling capacity of the system. The thermoacoustic coefficient of performance (COP) and temperature differential of a helium-argon gas mixture at 1:1 proportion was evaluated using an experimental approach. Nylon 6 sheets of different arrangements were employed alongside various operating parameters such as cooling load (10W), frequency ($\lambda/4$, $3\lambda/4$, and $5\lambda/4$), and operating pressure (6 bar -10 bar). Reported research implies that adding helium-argon gas to thermoacoustic refrigeration (TAR) may improve their performance, expanding refrigeration and cooling applications. This mixture also reduced the onset temperature for thermoacoustic action, saving energy. According to experiments, the appropriate combination of these gases can outperform pure gas systems, making sustainable cooling possible. The study shows that the Honeycomb stack arrangement outperforms others in temperature regulation and cooling load capacity, especially at high pressures. Stack material gives significant results on the cooling performance of TAR, having the highest COP of 0.498. At 10 bar, the Honeycomb stack has the lowest cold-end temperature, while the Parallel stack has the highest at 6 bar. Linearity exists between cooling load and temperature differential, with Honeycomb stacks having the best cooling capacity at drive Pressure Ratio 10. The study reveals that Honeycomb stacks perform best in thermoacoustic refrigeration systems at more excellent pressure ratios.*

## 1.0 INTRODUCTION

Thermoacoustic cooling uses no hazardous refrigerants and is environmentally friendly[1]. A resonator or cooling chamber uses sound waves and thermal reactions for thermoacoustic cooling [2]. Acoustic waves—gas pressure waves—drive this process. These waves' compression and rarefaction cycles induce rapid temperature and pressure changes[3]. Thermoacoustic cooling relies on the oscillation of thermal acoustic coolers to cause cooling. The system comprises resonators, stacks, and heat exchangers [4]. A tube or cavity resonator amplifies acoustic waves at specific frequencies and transfers energy to the gas medium [5]. The cooling

***HOW TO CITE:***
Shelke, K. S., Wankhede, U. S., and Shelare, S. "Thermoacoustic Cooling Performance using Nylon 6 Stack Material of Varied Geometry and Blended Helium-Argon Gas", *Nigerian Journal of Technology*, 2025; 44(1), pp. 77 – 86; *https://doi.org/10.4314/njt.v44i1.9*

process depends on the resonator stack, which is often porous or structured. The gas particles oscillate in response to sound waves, amplifying the interaction between thermal energy and acoustic phenomena [6]. As the gas compresses, particles heat up at high pressure while they cool during expansion at low pressure[7]. The net heat transfer during oscillation reduces the temperature of the stack[8]. Heat exchangers are placed at both ends of the stack to aid in the absorption and release of ambient thermal energy. Several variables, such as resonator design, gas type, stack material, and geometry, affect the system's efficiency. The speed of sound and the overall cooling process efficiency are affected by the gas selection. Numerous thermoacoustic devices utilize helium and argon. Since argon has a higher molecular weight, it absorbs and transfers heat better than helium, which propagates sound faster[9]. Mixtures of these gases improve system performance. Thermoacoustic cooling has many advantages over conventional cooling. It works without hazardous refrigerants and has fewer moving parts, reducing maintenance and improving system reliability. Acoustic energy optimization using thermoacoustic systems can reduce energy consumption, especially in heat transfer applications.

The stack is essential for heat transfer through gas particle oscillation in thermoacoustic systems. Thermal, acoustic performance and efficiency rely on stack material and shape[10]. These elements determine the system's ability to convert acoustic energy into thermal energy and cool. The stack material must meet thermal, acoustic, and mechanical requirements for system efficiency. To maintain an adequate stack temperature difference, the material must have moderate thermal conductivity, as heat transfer is inefficient if the substance conducts heat too quickly or poorly [11]. Since the stack must transmit sound waves without dampening, the material's acoustics are crucial. High porosity and surface area materials improve gas particle-stack interaction and heat transfer [12]. To ensure stability under repeated heating, cooling cycles, and fluctuations in acoustic wave pressure, the material must maintain mechanical integrity. Nylon 6 is selected for stack designs due to its equilibrium of thermal conductivity, mechanical strength, and acoustic properties [13]. Polycaprolactam, or nylon 6, is a semicrystalline polyamide. Nylon 6 is a peculiar case when comparing condensation and addition polymers since it is generated by ring-opening polymerization, unlike most other nylons. Durable, elastic, and shiny, Nylon 6 fibers are ideal for various applications. They defy wrinkling and are impervious to substances like acids and alkalis and abrasion. Nylon 6 has a glass transition temperature of 47 °C. Its density is 1.14 g/cm$^3$, and its tenacity is 6-8.5 gf/D. On average, it can withstand temperatures up to 150 °C, and its melting point is 215 °C. A precisely constructed stack of Nylon 6 sheets was employed to investigate the impact of porosity ratio and gap size on the performance of thermoacoustic refrigeration systems. The stack geometry is another factor that goes into determining the cooling performance.

Different arrangements like flat plates, tubes, and honeycomb shapes have advantages and disadvantages regarding surface area and gas flow. Correctly managing the spaces between stack layers or pores is important for getting the best gas-particle and stack wall interactions [14]. The ideal spacing should align with the gas's thermal penetration depth. Cooling efficacy also depends on stack length, thickness, and cross-sectional area. Although it increases acoustic losses, a longer stack increases temperature gradient and cooling power [15]. A thinner stack facilitates heat transfer, though it must remain structurally sound to withstand pressure changes. Strategic placement within the resonator, where acoustic pressure is high, and gas velocity is moderate, optimizes gas-particle-wall interactions. An optimal material and design that maximizes surface area without restricting gas flow can increase cooling efficiency, whereas a poor combination can lower system performance [16], [17]. So stack material and shape are key to thermoacoustic cooling system efficiency. Heat transfer and cooling are optimized by stack design and material properties like thermal conductivity and acoustic transparency. These considerations make the stack essential for creating advanced thermoacoustic cooling systems.

Hofler's thermoacoustic refrigerator cools by generating a standing wave in the resonator and using a regenerator like its stack of plates/screens. Many refrigeration and cooling applications could benefit from this promising gadget. Figure 1 shows the thermoacoustic refrigerator stack's middle position. This stack is essential to heat transfer in a closed resonator tube's inert gas environment. Both stack ends have heat exchangers to support their function. Thermal exchangers are made of copper hollow tubes with 2 and 4-millimetre diameters. Heat is transferred efficiently by these tubes in the thermoacoustic refrigerator. Copper mesh having 0.6 millimeters thickness and an estimated 80% porosity ratio improves heat transfer between the two heat exchangers, optimizing system efficiency. For thermoacoustic refrigerator structural components

like the resonator, nylon 66 is used. Due to its insulation and ease of manufacturing, it is a feasible alternative for system elements.

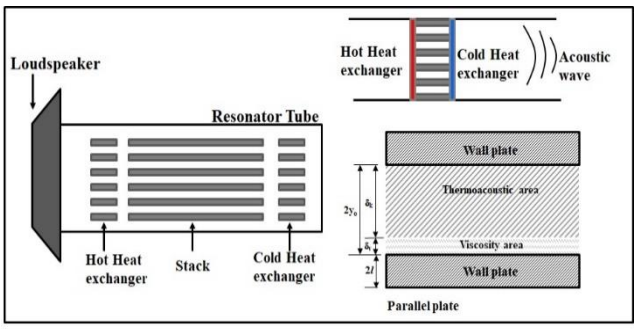


**Figure 1:** Schematic diagram of a typical thermo-acoustic refrigerator

The efficiency, acoustics, and cooling efficacy of thermoacoustic systems are significantly influenced by the working gas [18]. Combining different behaving helium and argon enhances the cooling performance. In thermoacoustic devices, sound waves compress and rarefy the gas [19]. Heat transfer during temperature oscillations is influenced by the speed of sound, thermal conductivity, specific heat ratio, and density[20]. Helium accelerates acoustic energy transfer due to its faster sound wave propagation. Increasing temperature variations and heat transfer rates enhance cooling efficacy [21]. High thermal conductivity helps helium absorb and release heat during stack oscillations. Low-density helium reduces viscosity and energy losses, improving system efficiency [22]. In conjunction with helium, argon plays a vital role in thermoacoustic systems. Argon's increased density accelerates cooling and holds more heat per volume than helium, improving heat transfer [23]. Additionally, due to its moderate thermal conductivity, argon enhances cooling and avoids premature heat dissipation by increasing the temperature gradient [24]. Argon's heat absorption and helium's fast sound propagation optimize cooling and acoustics [25]. Adjusting the helium-argon ratio can further improve thermoacoustic cooling efficiency. Nevertheless, the high cost and leakage of helium make it challenging to maintain the equilibrium of these gases. Despite these obstacles, helium-argon mixtures are frequently implemented in a variety of scientific and medical devices, refrigeration, HVAC systems, and cryogenic cooling [26]. Although adjusting the gas composition and managing helium leakage is complex, the mixture's acoustic and thermal properties make it an effective and environmentally friendly solution to improve thermoacoustic cooling systems.

The selection of the working gas, which transmits and stores the acoustic energy, affects the efficacy of thermoacoustic devices [27]. Thus, heat-driven thermoacoustic refrigerator operating gas efficiency must be assessed. Giacobbe et al. [28] calculated gas combination Prandtl numbers in 1994 to help choose working gases for thermoacoustic refrigerators. Later, in 1999, Jin et al. used Giacobbe's linear thermoacoustic theory method to investigate the impact of mixed gases on the performance of thermoacoustic refrigerators. Their findings suggested that low Prandtl numbers and acoustic velocities enhance the thermoacoustic energy conversion efficiency [29], [30].

Tijani's [31] study showed that reducing the Prandtl number of gases enhanced the performance of thermoacoustic refrigerators. In a follow-up study, Belcher et al. [32] examined the impact of specific heat ratio and Prandtl number on the onset temperature of thermoacoustic engines. They found that a low specific heat ratio and larger Prandtl number lower these engines' onset temperature. He et al. [33] found that working gases like helium and nitrogen alter pressure amplitude and frequency in solar-powered thermoacoustic engines 2009. Chen et al. [27] found that helium's performance in small-scale thermoacoustic Stirling engines is less sensitive to system factors than nitrogen and argon. Dong et al. [34] found that helium outperforms nitrogen and argon in large-scale thermoacoustic Stirling engines at mean pressures from 0.4 to 2.6 MPa. A compact thermoacoustic refrigerator with two electroacoustic components and one core is designed by Ramadan et al. [35]. The investigation furnishes comprehensive details regarding the fabrication, design, and testing procedures. The study examined the influence of driver piston displacement amplitude on performance indices. The DeltaEC design model and prototype function similarly, although non-linear factors lead to differences in performance. A two-unit thermoacoustic refrigerator for room-temperature cooling uses medium- and low-grade thermal energy developed by Chi et al. [36]. The system resonates efficiently with slender tubes and cavities. Experimental heat-driven thermoacoustic refrigera-tors have a minimal onset temperature of 64°C, cooling power from 0.66 kW to 5.62 kW, and a power density of 14.95 kW/m3, the greatest ever.

A possible eco-friendly refrigeration option is thermoacoustic cooling, which uses fewer mechanical components and avoids hazardous refrigerants. The efficacy of these systems is contingent upon factors such as stack materials and geometry, which affect

acoustics and heat transmission. Although the effectiveness of different stack shapes is well-known, the precise impact of nylon 6 in conjunction with helium-argon gas is poorly understood. Research has concentrated on basic thermoacoustic concepts or specialized factors like gas types or simple stack shapes, neglecting the various stack geometries and material-specific properties like nylon 6. Additional research is required to investigate the interaction between helium-argon gas and nylon 6 geometries in thermoacoustic cooling systems. Although thermoacoustic technology is advancing, significant gaps remain in research. Studies explicitly addressing nylon 6 as a stack material are limited. Nylon 6 has good mechanical qualities and low heat conductivity, but its performance in different geometric forms is not fully understood. Most studies have favored parallel plate configurations over cylindrical, triangular, or rectangular stack shapes, which could substantially affect the thermal and acoustic transfer. Although helium-argon blends are well known, the effects of combining different gas mixtures with complex stack designs for cooling have not been extensively studied. To maximize system efficiency, stack geometries have been studied extensively [9], [37], [38]. Spiral stacks with honeycomb architecture, circular stacks, and parallel plate stacks have pros and cons. These studies seek the best stack configuration for noise reduction, cooling power, and efficiency.

A thermoacoustic cooling system using helium-argon gas is tested using nylon 6 stack material of various shapes. The research examines thermoacoustic cooling utilizing cylindrical, rectangular, and triangular stack configurations. Total cooling efficiency, temperature drops, and heat transmission was discussed. The experiment investigates nylon 6's thermal and mechanical compatibility and cooling output by interacting with helium-argon gas. The cooling effectiveness of various geometries under-regulated gas and acoustic mixing was also compared. The optimal helium-argon ratio and geometrical designs of nylon 6 was also determined by the study. The stack material, form, and gas composition of industrial and commercial thermoacoustic systems was optimized last. The study investigates thermoacoustic system cooling with nylon 6 stacks of various geometries and helium-argon gas to fill these gaps.

## 2.0 EXPERIMENTAL SETUP AND PROCEDURE SPECIFICATIONS

The Hofler Thermoacoustic Refrigerator system was utilized, as shown in Figure 1. This novel cooling system uses thermoacoustics. The thermoacoustic refrigerator's resonator is a cylindrical metal tube. A thermoacoustic refrigeration resonator with two sealed ends holds helium or air. Two heat exchangers maintain fluid temperature by transferring heat to and from it. Heat transmission in the resonator is optimized by copper plates/screens. Transducers generate standing waves that compress and expand fluid, causing thermoacoustics. Compression heats the liquid at the hot end, and expansion cools it at the cold end, improving system efficiency.

A thermoacoustic refrigerator experimental setup includes numerous critical components, as shown in Figure 2. The resonator, heat exchanger, regenerator, driver, and measurement and control system are included. The system's vital resonator houses the working fluid and creates a stationary acoustic wave. Resonators have two ends, the hot and cold ends, made of metal or ceramic. Secure sealing prevents working fluid leaks.


**Figure 2:** Experimental setup of thermoacoustic refrigerator

The regenerator stores and releases thermal energy during the compression and expansion cycles within the resonator. It uses a porous material, such as ceramic or wire mesh, which is designed to have a large surface area to facilitate efficient thermal conduction. The resonator is energized by a continuous acoustic wave generated by the motor. A loudspeaker with a maximum power of 15 watts and an impedance of 10 ohms at functional occurrence (500Hz) was utilized as an acoustic driver. The loudspeaker was driven by a signal creator and power amplifier. A measuring and control system monitors and controls the thermoacoustic refrigerator. The charging pressure is measured by a Bourdon tube pressure gauge, as indicated in the experimental setup diagram. For measuring temperature in hot and cold heat exchanges, thermocouples are employed. Data is collected, analyzed, and stored on a computer or similar device to precisely regulate the thermoacoustic refrigerator's functioning. In the experimental set-up,

the nomenclature (1) shows speaker assembly, (2) shows flange, (3) shows stack holder, (4) shows resonator tube, (5) shows buffer volume, (6) shows heat exchanger, (7) shows temperature indicator, (8) shows high-pressure gauge, and (9) shows low-pressure gauge.

Figure 3 shows the various shapes of the stack. The cooling load was 10 watts, the frequency was λ/4, 3 λ/4, and 5 λ/4, and the operating pressure between 6 and 10 bars were among the other parameters to evaluate these stacks.
This study illuminates how porosity ratio and gap size affect thermoacoustic refrigerator performance. Understanding these components' physics helps researchers develop more efficient and dependable thermoacoustic refrigeration methods. Advances in cooling technology can reduce environmental impact and meet the growing need for efficient cooling systems.


**Figure 3:** Various stack geometries **(a)** spiral, **(b)** parallel, and **(c)** honeycomb

A series of experiments were conducted using different operational scenarios and stack geometries to determine how plate spacing affects thermoacoustic refrigerator performance, particularly temperature differentials. To enable these studies, the thermoacoustic refrigerator's resonating system had a pressure regulation system that adjusted working pressures from 6 to 10 bar. Helium, argon, and their mixture at a 1:1 ratio can be used due to their flexibility. All experimental measurements were conducted at 500 Hz to guarantee homogeneity.
The cold heat exchanger is connected to the resistance heating coil powered by the 5A30V DC power supply, enabling cooling. The system stabilizes, maintaining operational pressure, and data collecting begin each experimental session. To fully assess performance, each experiment tests various average cooling loads, operating pressures, driving ratio combinations, and operating frequencies.

This structured approach ensures that the studies are controlled and consistent, allowing for a precise evaluation of how variations in plate spacing within the stack influence the performance of the thermoacoustic refrigerator. These experiments could improve energy-efficient and environmentally friendly cooling technologies by informing thermoacoustic refrigeration system design and optimisation.

## 3.0 RESULTS AND DISCUSSION

Figure 4 shows the 500-Hz correlation between cold-end temperature and pressure across stack configurations. Spiral, Parallel, and Honeycomb architectures have different temperatures, as shown by the graphs. Specific temperature changes are 8–20 degrees Celsius for Spiral, 9–24 degrees Celsius for Parallel, and 2–16 degrees for Honeycomb structures. At 6 bar pressure, the Parallel structure has a maximum temperature of 28 degrees Celsius. At 10 bar pressure, the Honeycomb structure has the lowest temperature, 2 degrees Celsius. These results illuminate stack configuration performance.

Honeycomb structure leads to temperature control, especially under high pressure. Conversely, the Parallel structure achieves higher temperatures, especially at low pressure. These tips help optimize stack configurations for thermoacoustic refrigeration, improving temperature control and system efficiency.

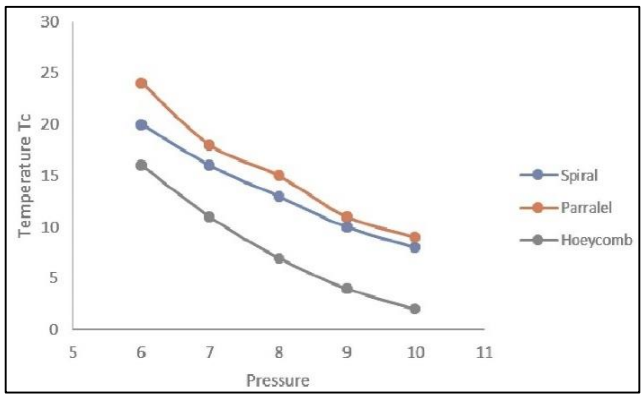


**Figure 4:** Cold end stack temperature vs pressure at 500 Hz for diverse stack geometries

Experimentation data shows that the honeycomb structure performs better with different stack geometries and cooling loads. The honeycomb structure consistently has the lowest cold-end temperatures of all geometries, making it a promising choice for improving Thermoacoustic Refrigerators.

Figure 5 shows how pressure affects the stack's hot end temperature, sustaining a constant frequency and cooling load. The significant difference in temperature is around 4 bars in the investigated pressure range. Beyond this limit, raising pressure reduces the

temperature difference, showing that air compression doesn't cool. These findings demonstrate that thermally activated refrigerators (TARs) have an ideal pressure range for maximum temperature differentials. Engineers can improve TAR system efficiency and efficacy by identifying the optimal pressure range. These discoveries enlighten the physics of thermoacoustic refrigeration and contribute to enhancing performance and design.

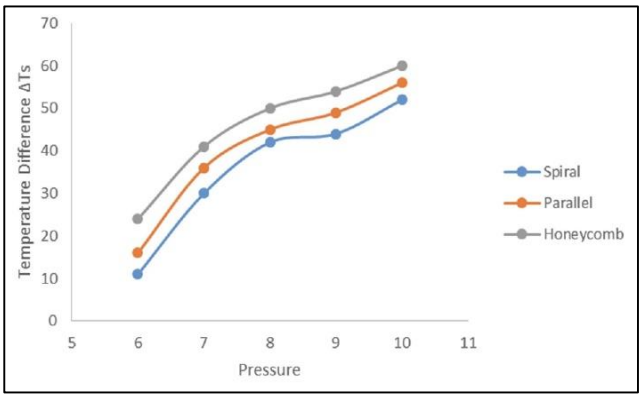


**Figure 5:** Hot end stack temperature difference vs pressure at 500 Hz for diverse stack geometries

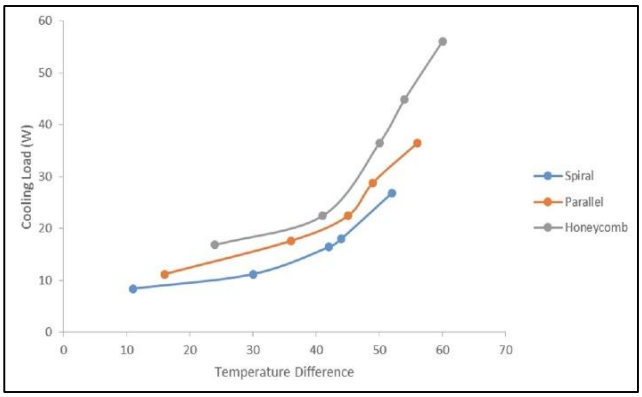


**Figure 6:** Stack geometry impact on cooling load and temperature difference

Figure 6 shows how the cooling load and stack temperature differential relate. The graph demonstrates a similar relationship between the temperature gap and cooling load, indicating that the temperature difference across the hot and cold sides of the stack increased correspondingly as the cooling load increased. These uncertainties show the imprecision of cooling load measurements and computations. Despite these uncertainties, the graph demonstrates a linear cooling load-temperature gap relationship.

These insights are essential for thermoacoustic refrigerator development and use. Knowledge of cooling load and temperature gaps helps engineers improve system performance. This study exposes thermoacoustic refrigeration fundamentals and may help this burgeoning industry build more accurate and efficient systems.

TAR and charging pressure mean COP are shown in Figure 7. In testing, honeycomb stacks reached 0.498 COP. Charging pressure changes affect the system, as demonstrated by COP fluctuations.

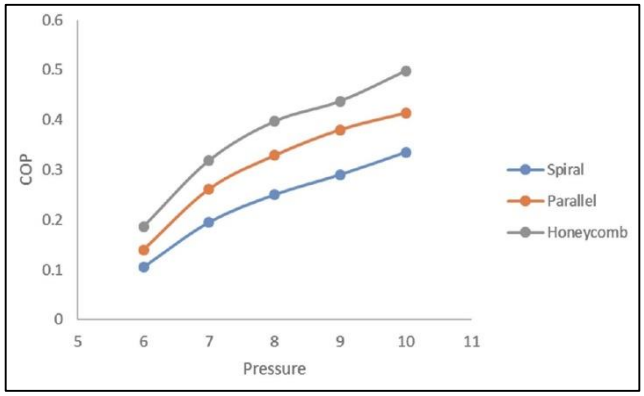


**Figure 7:** Charging pressure and stack geometry affect COP

A COP of 0.43 may seem low compared to conventional vapor compression refrigeration systems, but thermoacoustic refrigerators (TARs) have unique performance characteristics and are still in development. Vapor compression devices have lower COPs than thermoacoustic cooling.

A Thermal Absorption Refrigeration (TAR) system with a COP of 0.498 can cool efficiently and sustainably [37]. These technologies could become more efficient and commercially viable with more research and development. These findings lighten TAR performance and open the path for more eco-friendly and efficient cooling methods.

Figure 8 shows the cooling load grows substantially for all setups as the drive pressure ratio approaches 7. The Parallel and Spiral stacks climb moderately to 11 W and 20 W, respectively, while the Honeycomb stack leads with 25 W. With a slight increase in drive pressure ratio, all designs improve cooling performance dramatically. Between drive pressure ratios 8 and 10, all configurations' cooling load increases slowly. Honeycomb stacks have the most enormous cooling load, 52 W, with a Drive Pressure Ratiodrive pressure ratio of 10. The spiral stack gets 29 W, and the Parallel stack gets 38 W. The Honeycomb stack beats the other layouts in cooling capacity, especially at higher pressure ratios. For cooling load capacity across drive pressure ratios, the Honeycomb structure is best, especially at higher

ratios. At larger ratios, the Parallel stack improves and becomes more efficient. Spiral stacks start with the lowest cooling load but improve consistently, reaching comparable results to Parallel stacks at more significant pressures.

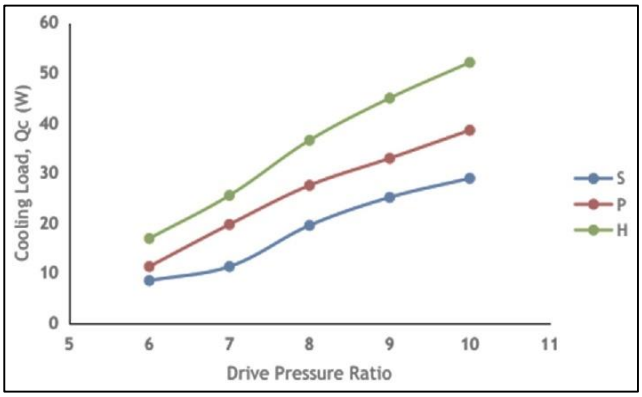


**Figure 8:** Effect of drive pressure ratio on cooling load of the system, helium-argon as a working fluid

Higher drive pressure ratios improve efficiency in all setups, albeit at different rates, as shown in Figure 9. Since the Honeycomb stack increases COP the greatest, it may be the best option for high-pressure applications. Although improving, the Spiral stack is less efficient than the other variants. The Honeycomb stack has a higher COP when helium is employed as the working fluid.

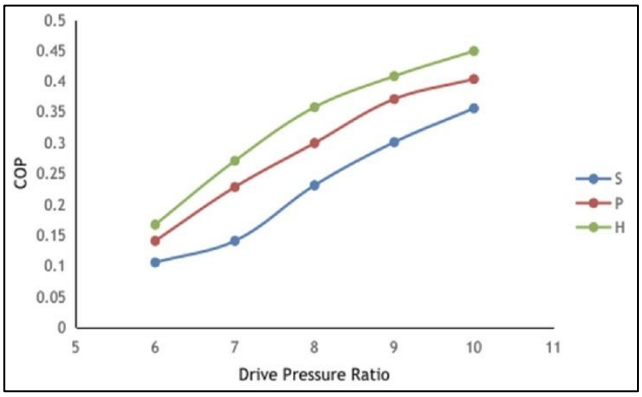


**Figure 9:** Effect of drive pressure ratio on COP of the system, helium-argon as a working fluid

Figure 10 shows the Coefficient of Performance (COP) of Helium (He) and Helium-Argon (HA) gases across Spiral (S), Parallel (P), and Honeycomb (H) stack geometries as a function of driving pressure ratio. The COP on the y-axis measures cooling efficiency, while the drive pressure ratio on the x-axis shows the system pressure differential. Helium-Argon (HA) COP grows gradually with the drive pressure ratio in all geometries. The Honeycomb arrangement (H-HA) has the maximum efficiency, with COP near 0.43 at a 10-driving pressure ratio. The Parallel configuration (S-HA) performs next best with a COP of 0.40, while the Spiral configuration (P-HA) performs worst with 0.35.

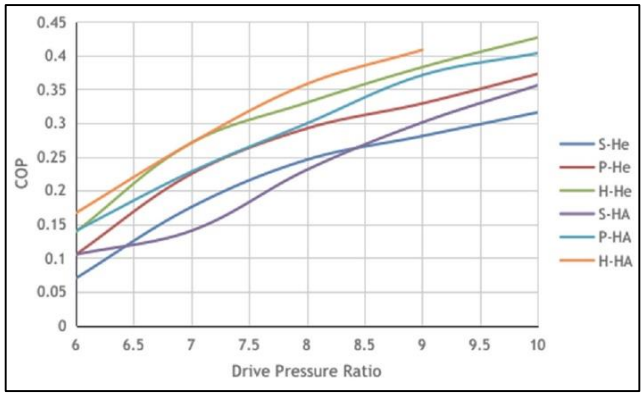


**Figure 10:** Comparison of COP of the different stacks geometry for Helium and Helium-Argon gas

Figure 11 compares actual and DeltaEC simulation results for helium-argon mix working fluid temperature change (ΔT) at various pressures. Pressure raises the difference in temperature, as shown by both experiments and Simulations. Simulations diverge slightly from experimental data. Experimental data and simulation models differ somewhat. Higher pressures raise temperature differences for the thermoacoustic cooling system's helium-argon blend, stacked in nylon 6.

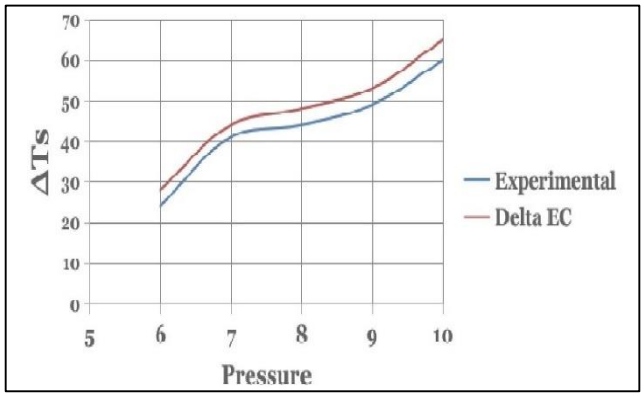


**Figure 11:** Simulation of experimental data with DeltaEC software

## 4.0 CONCLUSION

The study evaluates various stack geometries and cooling loads, as well as the impact of charging pressures and drive pressure ratios on the efficiency of the thermoacoustic refrigeration (TAR) system. The key conclusions obtained by the study are:

- The cooling load increases with the drive pressure ratio, and the Honeycomb stack outperforms the spiral and parallel stacks.
- At a 10:1 drive pressure ratio, the Honeycomb

stack achieved the highest cooling load of 52W.

- The Coefficient of Performance (COP) also increases with pressure ratios, with the Honeycomb configuration showing the highest.
- The Honeycomb structure consistently achieved the lowest cold-end temperatures, indicating its cooling efficiency.
- Higher pressures improve temperature differences, supporting the experimental findings.
- Optimizing stack configurations, pressure ratios, and helium-argon use can enhance the cooling capacity and efficiency of thermoacoustic refrigeration systems.

## REFERENCES


[1] Akinsade, A., Eiche, J. F., Akinola, A. O., and Famodun, M. O. "Conceptual design and analysis of a tricycle mounted solar-powered photovoltaic cold room system," *Niger. J. Technol.*, vol. 42, no. 4, pp. 457–463, Feb. 2024, doi: 10.4314/njt.v42i4.5.

[2] Ali, U., Al-Mufti, O., and Janajreh, I. "Harnessing sound waves for sustainable energy: Advancements and challenges in thermoacoustic technology," *Energy Nexus*, vol. 15, p. 100320, 2024, doi: https://doi.org/10.1016/j.nexus.2024.100320.

[3] Mogaji, T. S., Awolala, A., Ayodeji, O. Z., Mogaji, P. B., and Philip, D. E. "COP enhancement of vapor compression refrigeration system using dedicated mechanical subcooling cycle," *Niger. J. Technol.*, vol. 39, no. 3, pp. 776–784, Sep. 2020, doi: 10.4314/njt.v39i3.17.

[4] Hou, Z., Li, N., Huang, X., Li, C., Lv, H., Kang, Y., and Weng, C. "Experimental study on pressure evolution of detonation waves penetrating into water," *Phys. Fluids*, vol. 34, no. 7, Jul. 2022, doi: 10.1063/5.0100446.

[5] Nwankwo, E. J. "Development and evaluation of a cost-effective aeration-filtration solar disinfection system for water treatment," *Niger. J. Technol.*, vol. 43, no. 4, pp. 779–787, 2024.

[6] Ozigis, I. I., Lawal, M. N., Nnaji, C. C., and Akpan, P. "Characterization of petrol, ethanol and spent engine oil blends for twostroke single-cylinder spark-ignition engine," *Niger. J. Technol.*, vol. 43, no. 3, pp. 470–478, 2024, doi: https://doi.org/10.4314/njt.v43i3.9.

[7] Uwadiae, M. E., Akintunde, M. A., and Ogedengbe, T. I. "Experimental investigation of R-134a and R-600a refrigerant blend in domestic vapour compression refrigeration system," *Niger. J. Technol.*, vol. 36, no. 4, p. 1138, 2018, doi: 10.4314/njt.v36i4.20.

[8] Frank, E., and Effiom, S. O. "Development of a Multigeneration System With Integrated Hydrogen Production: a Typical Analysis," *Niger. J. Technol.*, vol. 42, no. 3, pp. 330–338, 2023, doi: 10.4314/njt.v42i3.5.

[9] Siva Sakthi, M., Swathiga Devi, C., and Bogadi, S. "Design and Analysis of a Thermoacoustic Cooling System with Two-Stack Arrangement for Different Types of Stacks BT - Advances in Mechanical Engineering and Material Science," in *In: Tambe, P., Huang, P., Jhavar, S. (eds) Advances in Mechanical Engineering and Material Science. ICAMEMS 2023. Lecture Notes in Mechanical Engineering. Springer, Singapore.*, Tambe, P., Huang, P., and Jhavar, S. Eds., Singapore: Springer Nature Singapore, 2024, pp. 69–84.

[10] Bouramdane, Z., Bah, A., Alaoui, M., and Martaj, N. "Numerical analysis of thermoacoustically driven thermoacoustic refrigerator with a stack of parallel plates having corrugated surfaces," *Int. J. Air-Conditioning Refrig.*, vol. 30, no. 1, p. 1, Dec. 2022, doi: 10.1007/s44189-022-00002-8.

[11] Zheng, Q., Hao, M., Miao, R., Schaadt, J., and Dames, C. "Advances in thermal conductivity for energy applications: a review," *Prog. Energy*, vol. 3, no. 1, p. 012002, Jan. 2021, doi: 10.1088/2516-1083/abd082.

[12] Zhang, K., Du, S., Sun, P., Zheng, B., Liu, Y., Shen, Y., Chang, R., and Han, X. "The effect of particle arrangement on the direct heat extraction of regular packed bed with numerical simulation," *Energy*, vol. 225, p. 120244, 2021, doi: https://doi.org/10.1016/j.energy.2021.120244.

[13] Tao, Y., Ren, M., Zhang, H., and Peijs, T. "Recent progress in acoustic materials and noise control strategies – A review," *Appl. Mater. Today*, vol. 24, p. 101141, 2021, doi: https://doi.org/10.1016/j.apmt.2021.101141.

[14] da Silva, J. D., Moreira, D. C., and Ribatski, G. "An overview on the role of wettability and wickability as a tool for enhancing pool boiling heat transfer," Abraham, J. P., Gorman, J. M., and W. B. T.-A. in H. T. Minkowycz, Eds., Elsevier, 2021, pp. 187–248. doi: 10.1016/bs.aiht.2021.06.003.

[15] Kayes, M. I., and Rahman, M. A. "Experimental investigation of a modified parallel stack for wet thermoacoustic engine to improve performance and suppress harmonics,"

*Appl. Acoust.*, vol. 212, p. 109569, 2023, doi: https://doi.org/10.1016/j.apacoust.2023.109569.

[16] Gassar, A. A. A., Koo, C., Kim, T. W., and Cha, S. H. "Performance Optimization Studies on Heating, Cooling and Lighting Energy Systems of Buildings during the Design Stage: A Review," *Sustainability*, vol. 13, no. 17, p. 9815, Sep. 2021, doi: 10.3390/su13179815.

[17] Ganvir, V., Belkhode, P., Kurve, A., Shelare, S., Maheshwary, P., Sharma, S., Dwivedi, S.P., Kumar, S., Bisht, Y. S., and Abbas, M. "Green energy using oscillatory baffled reactors: advances in biodiesel production from high free fatty acid karanja oil," *Int. J. Chem. React. Eng.*, vol. 22, no. 9, pp. 1107–1122, Sep. 2024, doi: 10.1515/ijcre-2024-0051.

[18] Xiao, L., Luo, K., Wu, Z., Chi, J., Xu, J., Zhang, L., Hu, J., and Luo, E. "A highly efficient heat-driven thermoacoustic cooling system," *Cell Reports Phys. Sci.*, vol. 5, no. 2, Feb. 2024, doi: 10.1016/j.xcrp.2024.101815.

[19] Griffin, J. M., Jones, S., Perumal, B., and Perrin, C. "Investigating the Detection Capability of Acoustic Emission Monitoring to Identify Imperfections Produced by the Metal Active Gas (MAG) Welding Process," *Acoustics*, vol. 5, no. 3. pp. 714–745, 2023. doi: 10.3390/acoustics5030043.

[20] Di Meglio, A., Di Giulio, E., Dragonetti, R., and Massarotti, N. "Analysis of heat capacity ratio on porous media in oscillating flow," *Int. J. Heat Mass Transf.*, vol. 179, p. 121724, 2021, doi: https://doi.org/10.1016/j.ijheatmasstransfer.2021.121724.

[21] Eanest Jebasingh, B., and Valan Arasu, A. "A detailed review on heat transfer rate, supercooling, thermal stability and reliability of nanoparticle dispersed organic phase change material for low-temperature applications," *Mater. Today Energy*, vol. 16, p. 100408, 2020, doi: https://doi.org/10.1016/j.mtener.2020.100408.

[22] Ghorbani, B., and Amidpour, M. "Energy, exergy, and sensitivity analyses of a new integrated system for generation of liquid methanol, liquefied natural gas, and crude helium using organic Rankine cycle, and solar collectors," *J. Therm. Anal. Calorim.*, vol. 145, no. 3, pp. 1485–1508, 2021, doi: 10.1007/s10973-021-10659-9.

[23] Zhang, R., Zhang, X., Qing, S., Luo, Z., and Liu, Y. "Investigation of nanoparticles shape that influence the thermal conductivity and viscosity in argon-based nanofluids: A molecular dynamics simulation," *Int. J. Heat Mass Transf.*, vol. 207, p. 124031, 2023, doi: https://doi.org/10.1016/j.ijheatmasstransfer.2023.124031.

[24] He, Z., Yan, Y., and Zhang, Z. "Thermal management and temperature uniformity enhancement of electronic devices by micro heat sinks: A review," *Energy*, vol. 216, p. 119223, 2021, doi: https://doi.org/10.1016/j.energy.2020.119223.

[25] Mohebbifar, M. R. "Optical measurement of gas vibrational-translational relaxation time with high accuracy by the laser photo-acoustic set-up," *Microchem. J.*, vol. 164, p. 106040, 2021, doi: https://doi.org/10.1016/j.microc.2021.106040.

[26] Ismail, M., Yebiyo, M., and Chaer, I. "A Review of Recent Advances in Emerging Alternative Heating and Cooling Technologies," *Energies*, vol. 14, no. 2. 2021. doi: 10.3390/en14020502.

[27] Chen, M., and Ju, Y. L. "Effect of different working gases on the performance of a small thermoacoustic Stirling engine," *Int. J. Refrig.*, vol. 51, pp. 41–51, 2015, doi: https://doi.org/10.1016/j.ijrefrig.2014.12.006.

[28] Giacobbe, F. W. "Estimation of Prandtl numbers in binary mixtures of helium and other noble gases," *J. Acoust. Soc. Am.*, vol. 96, no. 6, pp. 3568–3580, Dec. 1994, doi: 10.1121/1.410615.

[29] Swift, G. W. "Thermoacoustics: A unifying perspective for some engines and refrigerators", *Springer*, 2017.

[30] Swift, G. W. "Thermoacoustic engines," *J. Acoust. Soc. Am.*, vol. 84, no. 4, pp. 1145–1180, Oct. 1988, doi: 10.1121/1.396617.

[31] Tijani, M. E. H., Zeegers, J. C. H., and de Waele, A. T. A. M. "Prandtl number and thermoacoustic refrigerators," *J. Acoust. Soc. Am.*, vol. 112, no. 1, pp. 134–143, Jul. 2002, doi: 10.1121/1.1489451.

[32] Belcher, J. R., Slaton, W. V., Raspet, R., Bass, H. E., and Lightfoot, J. "Working gases in thermoacoustic engines," *J. Acoust. Soc. Am.*, vol. 105, no. 5, pp. 2677–2684, May 1999, doi: 10.1121/1.426884.

[33] Shen, C., He, Y., Li, Y., Ke, H., Zhang, D., and Liu, Y. "Performance of solar powered thermoacoustic engine at different tilted angles," *Appl. Therm. Eng.*, vol. 29, no. 13, pp. 2745–2756, 2009, doi: https://doi.org/10.1016/j.applthermaleng.2009.01.008.

[34] Dong, S., Shen, G., Xu, M., Zhang, S., and An, L. "The effect of working fluid on the

performance of a large-scale thermoacoustic Stirling engine," *Energy*, vol. 181, pp. 378–386, 2019, doi: https://doi.org/10.1016/j.energy.2019.05.142.

[35] Ramadan, I. A., Bailliet, H., Poignand, G., and Gardner, D. "Design, manufacturing and testing of a compact thermoacoustic refrigerator," *Appl. Therm. Eng.*, vol. 189, p. 116705, 2021.

[36] Chi, J., Yang, Y., Wu, Z., Yang, R., Li, P., Xu, J., Zhang, L., Hu, J., and Luo, E. "Numerical and experimental investigation on a novel heat-driven thermoacoustic refrigerator for room-temperature cooling," *Appl. Therm. Eng.*, vol. 218, p. 119330, 2023, doi: https://doi.org/10.1016/j.applthermaleng.2022.119330.

[37] Rahpeima, R., and Ebrahimi, R. "Numerical investigation of the effect of stack geometrical parameters and thermo-physical properties on performance of a standing wave thermoacoustic refrigerator," *Appl. Therm. Eng.*, vol. 149, pp. 1203–1214, 2019, doi: https://doi.org/10.1016/j.applthermaleng.2018.12.093.

[38] Khan, M. I., Siddiqui, T. R., and Rahman, M. A. "Combined experimental and numerical study on the performance of thermoacoustic refrigeration system," 2019, p. 030022. doi: 10.1063/1.511586.